IEEE Access
Multidisciplinary ⋮ Rapid Review ⋮ Open Access Journal

Received November 30, 2021, accepted January 16, 2022, date of publication January 27, 2022, date of current version February 11, 2022.

Digital Object Identifier 10.1109/ACCESS.2022.3146854

Improved Differential Phase Detecting Optical Fiber Interferometer With a Low-Frequency Compensation Scheme

YINGJIE WU[1], CHURUI LI[1], HUANG TANG[1,2], BO JIA[1,2], AND CHAO WANG[1,2]
[1]Department of Materials Science, Fudan University, Shanghai 200433, China
[2]Dongguan Institute of Advanced Optical Fiber Technology, Dongguan 523808, China

Corresponding author: Chao Wang (wangchao@fudan.edu.cn)

This work was supported by the Science and Technology Commission of Shanghai Municipality under Grant 17DZ2280600.

ABSTRACT To overcome the poor low-frequency response sensitivity of differential phase detecting interferometer, an improved differential phase detecting optical fiber interferometer with a time domain low frequency compensation scheme is designed and implemented, effectively compensating the low frequency loss of the system by means of recursive accumulation method. Theoretical derivation and experimental verification are conducted in this paper. The experimental results indicate that the improved system can significantly enhance the amplitude of 10 Hz signal and signals with high fidelity can be obtained because the compensated system responds equally both to the high and low frequency signals. Further experiments in the buried pipelines monitoring reveal that the signal-to-noise ratio is obviously improved by 22 dB approximately compared with the traditional system. The positioning error of the proposed system is within ±20 m along a 40 km sensing fiber. The differential phase detection interferometer compensated by the proposed scheme has potential application in low-frequency fields such as seismic wave detection, hydrophones, sonar, pipeline monitor and geological detection.

INDEX TERMS Optical fiber sensors, optical interferometry, vibration measurement.

I. INTRODUCTION

Optical fiber sensing technology has developed explosively and received a great attention since it was proposed in the 1970s. As an important part of optical fiber sensing technology, optical fiber interferometer is widely applied to the detection of vibration, temperature, stress and other physical quantities due to the outstanding advantages of high sensitivity, low cost and immunity to electromagnetic interference [1]–[3].

Optical fiber interferometers are categorized according to the different structures as Michelson interferometer [4], Mach-Zehnder (M-Z) interferometer [5], [6], Fabry-Perot interferometer [7], Sagnac interferometer [8], [9], and several hybrid structures [10]–[12]. On the other hand, in terms of signal acquisition methods the interferometers can also be classified into direct phase detecting interferometer such as Michelson interferometer [4] and differential phase detecting interferometer including M-Z interferometer [5]. The former has higher sensitivity, whereas the latter, widely used in engineering application, has significantly higher stability and can eliminate the influence caused by temperature and environmental changes because of the symmetrical structure.

In recent years, the application of modified hybrid M-Z and Sagnac optical fiber sensing system has become promising in the field of vibration detection on account of the superiorities of great stability, geometric versatility, insensitivity to environmental changes and distributed deployment [8], [13], [14]. However, the amplitude of sensing signal obtained by the differential phase detecting interferometer is reduced as the signal frequency decreases and the low-frequency component is overwhelmed by the higher one. Therefore, in low frequency detection the differential phase detecting system performs poorly.

As the concerned frequency band of vibration detecting extends to lower frequency, the performance of detecting low frequency signal is severely affected by both the system structure and the background noise. There are few researches

The associate editor coordinating the review of this manuscript and approving it for publication was S. M. Abdur Razzak.

on improving the performance of optical fiber interferometer to detect low frequency signal. Although the research [15] suggests a frequency response smoothing processing in the differential phase detecting interferometer, it is too complicated and unable to implement real-time application to practical application. In addition, some studies [16] have used frequency-domain model identification techniques to estimate the frequency response of the wavelength modulation (WM) and then design a corresponding compensator. However, this kind of compensator is designed to fit in a specific WM and cannot be universally implemented in all situations.

In this paper, we design and implement an improved differential phase detecting optical fiber interferometer with a time domain low frequency compensation scheme. In order to improve the differential phase detecting interference sensing system's response to low frequency signal, a compensator is designed for increasing the low frequency signal components of the detection signal effectively and achieving real-time detection of high-fidelity signal. Investigation on the system characteristic of the compensated differential phase detecting interferometer is conducted. The theoretical derivation and performance in noisy environment of this compensation scheme are analyzed in theory and are verified experimentally in practical system. The experimental results show that the signal-to-noise ratio (SNR) is significantly improved compared with the traditional differential phase detecting system.

II. THEORY

A. PRINCIPLE OF M-Z AND SAGNAC HYBRID INTERFERENCE SYSTEM

The structure of the M-Z and Sagnac hybrid single-core feedback interferometer using a 3 × 3 coupler is shown in Fig. 1, which is a differential phase detecting interferometer.

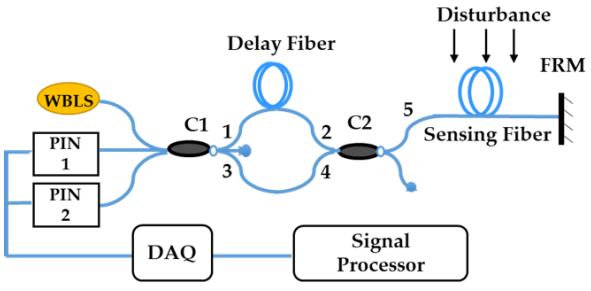

FIGURE 1. The schematic diagram of the hybrid M-Z and Sagnac interferometer consisting of wide band laser source (WBLS), Faraday rotator mirror (FRM), p-i-n photodiode (PIN), 3 × 3 coupler(C1), 2 × 2 coupler(C2) and data acquisition (DAQ).

The main light paths transmitting in the structure are as follows:

A: WBLS-3-4-5-FRM-5-2-1-PIN
B: WBLS-1-2-5-FRM-5-2-1-PIN
C: WBLS-1-2-5-FRM-5-4-3-PIN
D: WBLS-3-4-5-FRM-5-4-3-PIN

Due to the employment of wide band laser source with low coherence length, the length of the fiber delay line (FDL) is much longer than the coherence length of the laser source. Consequently, although the light coming out from the WBLS would be split into four paths in this structure, only the light beam A and beam C with the same path length interfere at the 3 × 3 coupler C1.

According to the photoelastic effect, the stress exerting on the optical fiber will be translated into the optical fiber changes of length and refractive index, and the phase change of the transmitted light is proportional to the stress. Therefore, the phase change of the interference light reflects the vibration information availably.

The interfered light of beam A and beam C is detected by PIN1 and PIN2 and are expressed as:

$$I_1(t) = E_1\{1 + cos(\Delta\varphi(t) + \varphi_0)\} \quad (1)$$

$$I_2(t) = E_2\left\{1 + cos\left(\Delta\varphi(t) + \varphi_0 + \frac{2}{3\pi}\right)\right\} \quad (2)$$

where E_1 and E_2 are the amplitudes of the sensing light, $\Delta\varphi$ is the phase difference modulated by the vibration we are interested, φ_0 is the initial phase, and $2/3\pi$ is the phase difference introduced by the C1.

As the FDL employed in the system, there is a time difference when the beams A and C are modulated by the disturbed signal. Assuming the vibration signal applied on the fiber at a distant of L from the FRM as $g(t)$, the beam will be modulated twice by the external vibration in the process of transmission and reflection, and the time interval of the two modulations is $T=2nL/c$. The interfered signals $I_1(t)$ and $I_2(t)$ then enter into the phase demodulation system [17], [18], and the retrieved result is:

$$\Delta\varphi(t) = g(t) + g(t-T) - [g(t-\tau) + g(t-T-\tau)] \quad (3)$$

where τ is the time delay caused by FDL. And then the autocorrelation operation is employed on the two time-delay signals to obtain the vibration position.

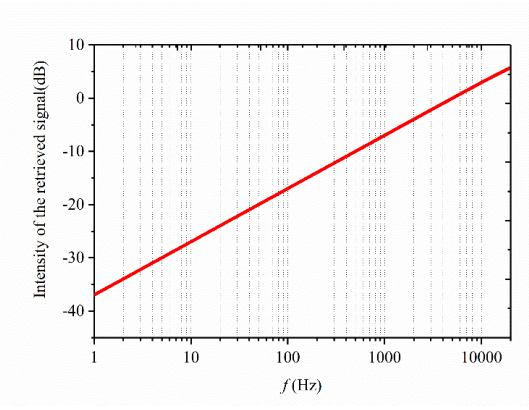

FIGURE 2. The frequency response of the differential phase detecting interferometer.

Assuming that the vibration signal is a single frequency signal, the phase modulation of the transmitted light is written as:

$$g(t) = \varphi_0 \sin \omega t \tag{4}$$

where φ_0 is the amplitude of the vibration signal and ω is the angular frequency of the vibration signal. Then (3) becomes [19]:

$$\begin{aligned}\Delta\varphi(t) &= \varphi_0 \sin \omega t + \varphi_0 \sin \omega (t - T) \\ &\quad -\varphi_0 \sin \omega (t - \tau) - \varphi_0 \sin \omega (t - T - \tau) \\ &= 4\varphi_0 \sin \frac{\omega\tau}{2} \cos\left(\frac{\omega T}{2}\right) \cos \omega \left(t - \frac{\tau + T}{2}\right)\end{aligned} \tag{5}$$

The amplitude A of the differential phase signal is proportional to the signal angular frequency ω as:

$$A(\omega) \propto \sin \frac{\omega\tau}{2} \tag{6}$$

The interference phase signal is the difference of the two terms of phase signals with a time delay difference τ. When τ is quite small (10^{-5}s is generally selected as the length of FDL does not exceed 2×10^3 m), the formula shows that the demodulated phase has a quite small amplitude in the low frequency band and increases with the augment of frequency. The impact term $\sin \frac{\omega\tau}{2}$ of the differential demodulation results is frequency dependent, which demonstrates the poor low-frequency response of the system during the vibration signal measurement. Taking the response at the frequency of 5 kHz as the 0 dB reference line, Fig. 2 is the frequency response of the differential phase detecting interference system in the frequency range of 1 Hz to 20 kHz. As shown in Fig. 2, the low-frequency components of the system are obviously small and overwhelmed by the high-frequency signals.

B. LOW-FREQUENCY SIGNAL COMPENSATION SCHEME

To tackle the problem of the poor low-frequency response in the above interferometer system, a time domain cumulative compensation scheme for the differential phase signal is proposed. To simplify, let $f(t) = g(t) + g(t - T)$ and the vibration signal we are concerned with is written as:

$$f(t) = \Delta\varphi(t) + f(t - \tau) \tag{7}$$

The time domain compensation scheme is a recursive accumulation algorithm, which will update the previous data and accumulate utilizing data within each time delay τ based on the previous accumulative results.

Considering that the signal is converted analog-to-digital in the system, the compensation algorithm will be described in discrete form. Suppose there are m discrete sampling points in τ s, in which a series of discrete times $t_{km+1}, t_{km+2}, \ldots, t_{km+m}, k = 0, 1, 2 \ldots$, corresponds to the step size $\Delta t = \frac{1}{f_s}$, and $\tau = m \cdot \Delta t$. On the more realistic assumption that the vibration signal is finite with data length of $n_f \cdot m$, the discrete time interval can be divided into $[t_{km+1}, t_{km+m}], k = 0, 1, \ldots, n_f - 1$. For simplicity, considering the first sampling point in each time interval, the discrete form of (8) can be written as:

$$\begin{aligned} f[t_1] &= \Delta\varphi[t_1] + f\{t_1 - m \cdot \Delta t\} \\ f[t_{m+1}] &= \Delta\varphi[t_{m+1}] + f[t_1] \\ &\cdots \\ f[t_{km+1}] &= \Delta\varphi[t_{km+1}] + f[t_{km+1-m}] \end{aligned} \tag{8}$$

According to (9), as long as the value of the first time interval $\{f[t_1], f[t_m]\}$ is obtained, $\{f[t_{m+1}], f[t_{2m}]\}$ can be calculated from the initial value of the first time interval. And then $\{f[t_{m+1}], f[t_{2m}]\}$ is taken as the initial value of the next step. The approximate value of $f(t)$ at each discrete time point in the kth time interval is obtained by iteration. Notably, for an infinite signal with data length of $n_f \cdot m$, the recursion time is n_f. And the more times we accumulate, the more stable the compensation results are.

The essential of recursion is the determination of initial conditions, that is, to determine the value of the first interval $\{f[t_1], f[t_m]\}$:

$$\begin{aligned} f[t_1] &= \Delta\varphi[t_1] + f[t_1 - m \cdot \Delta t] = \varphi[t_1] + C_1 \\ f[t_2] &= \Delta\varphi[t_2] + f[t_1 - (m+1) \cdot \Delta t] \\ &= \Delta\varphi[t_2] + C_2 \\ &\cdots \\ f[t_m] &= \Delta\varphi[t_m] + f[t_1 - 2m \cdot \Delta t] \\ &= \Delta\varphi[t_m] + C_m \end{aligned} \tag{9}$$

To acquire the initial value of the first-time interval $\{f[t_1], f[t_m]\}$, it is necessary to ascertain the constants $C_1, C_2, \ldots, C_m$. In practical applications, for a finite signal with an onset time t_1, when $t < t_1$ and $f[t] = 0$, it is assumed that $C_1, C_2, \ldots, C_m$ are equal to zero. As a consequence, the compensation algorithm is written as the following:

$$f(t) = \sum_{i=0}^{n_f - 1} \Delta\varphi(t - i \cdot \tau), \quad t > i \cdot \tau \tag{10}$$

Consequently, we retrieve the vibration signal $f(t)$ from $\varphi(t)$ yielding the recursion algorithm. By comparing the power P_{sout} of the compensator output with the power P_{sin} of the retrieved phase before compensation, the power gain K of the compensation system can be deduced as follows:

$$P_{sin} = \frac{\omega}{2\pi} \int_0^{\frac{2\pi}{\omega}} \Delta\varphi^2(t) dt = \varphi_0^2 [1 - \cos(\omega\tau)] \tag{11}$$

$$P_{sout} = \frac{\omega}{2\pi} \int_0^{\frac{2\pi}{\omega}} f^2(t) dt = \frac{\varphi_0^2}{2} \tag{12}$$

$$K = \frac{P_{sout}}{P_{sin}} = \frac{2}{1 - \cos(\omega\tau)} \tag{13}$$

Given that the signal frequency is $\omega = 2\pi f$, the $K - f$ curve is shown in Fig. 3. It can be observed that the amplitude of the compensated low-frequency signal has been improved. In addition, the system amplitude gain K gradually decreases

with the increase of the signal frequency, which compensates for the system frequency response completely shown in Fig. 2. As a result, the enhancement effect of low frequency component ameliorates the low-frequency response of the differential phase detecting interferometer system.

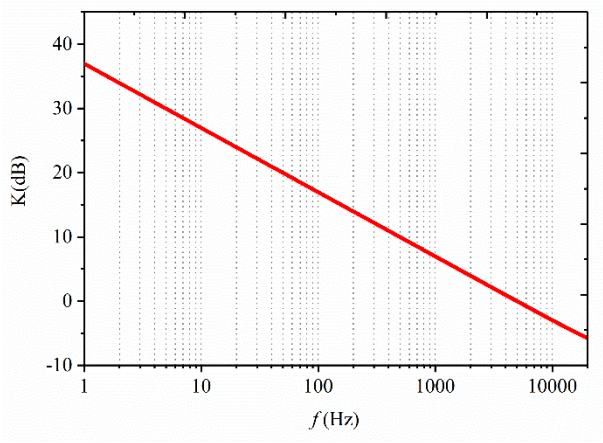

FIGURE 3. The K-f curve of the compensation system.

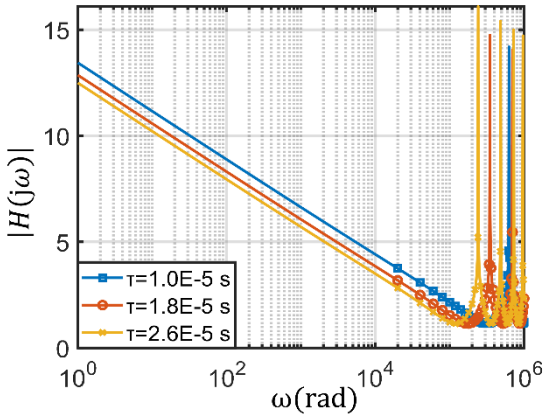

FIGURE 4. The amplitude-frequency response diagram of the compensation system.

It can be concluded from the (8) and (9) that the compensated phase signal becomes the phase modulation of the vibration signal, which offsets the differential phase in the original interference signal in (5). As a consequence, the amplitude of the compensated phase in the formula no longer changes with the vibration signal frequency. Therefore, the scheme realizes the flatness of various frequency bands response, revealing the low-frequency components that are originally overwhelmed by the high-frequency signals.

C. TRANSFER FUNCTION OF THE COMPENSATED SYSTEM

It is necessary to analyze the characteristics of the phase detecting interferometer system with the compensation scheme. The ith cumulative signal $\Delta\varphi(t - i\tau)$ of the time domain compensator can be regarded as the convolution integral of $\Delta\varphi(t)$ and the impulse function $\delta(t - i\tau)$:

$$\Delta\varphi(t - i\tau) = \Delta\varphi(t) * \delta(t - i\tau). \tag{14}$$

The time domain compensator serves as a linear system with an input signal of $\Delta\varphi(t)$ and an output of $f(t)$.The frequency response function of the compensator is given by:

$$H(j\omega) = \frac{2\pi}{\int_{-\infty}^{+\infty}[\delta(t) - \delta(t - \tau)]\, e^{-j\omega t} dt} = \frac{2\pi}{1 - e^{-j\omega\tau}} \tag{15}$$

The amplitude-frequency response diagram of the compensation system is shown in Fig.4. Due to the characteristics of the system, a harmonic of frequency $1/\tau$ will be generated, which will be solved by adding a low-pass filter behind the compensator. And the demonstration of the time domain compensation for the system frequency response is shown as Fig. 5. Furthermore, it can also be seen from Fig. 4 that if the parameter τ set in the algorithm deviates from the actual generated time delay, the curves will shift but the slope of compensated frequency response will keep constant. Therefore, this deviation will not affect the frequency response of the system, which also proves the stability of the compensation algorithm.

D. THE COMPENSATED SYSTEM PERFORMANCE IN NOISY ENVIRONMENT

In practical application, the background noise is inevitable and its effect on the differential phase detecting interferometer is vital. Considering the environmental noise during signal detecting, the differential phase information after interference becomes:

$$\Delta\varphi'(t) = \Delta\varphi(t) + n(t) \tag{16}$$

where $n(t)$ is the environmental white noise as a random process. The compensation is carried out for the retrieved phase signal containing environmental noise:

$$f'(t) = \sum_{i=0}^{n_f-1} \Delta\varphi'(t - i\tau) = \sum_{i=0}^{n_f-1} \Delta\varphi(t - i\tau) + \sum_{i=0}^{n_f-1} n(t - i\tau) \tag{17}$$

We suppose the power spectral density of finite Gaussian white noise is $S_n(\omega) = \frac{N_0}{2}$. The power of the noise over the frequency range of -B to B is:

$$P_{nin} = \frac{1}{2\pi}\int_{-B}^{B} S_n(\omega)\, d\omega = \frac{N_0 \mathrm{B}}{2\pi} \tag{18}$$

Accordingly, the power of output noise from the time domain compensator is:

$$P_{nout} = \frac{1}{2\pi}\int_{-B}^{B} S_n(\omega)\, |H(j\omega)|^2\, d\omega = \frac{N_0\pi\,[1 - \cos(B\tau)]}{\tau \cdot \sin(B\tau)} \tag{19}$$

Combining (12) with (13) above, the signal-to-noise improvement ratio (SNIR) of the system is derived as:

$$\mathrm{SNIR} = \frac{\frac{P_{sout}}{P_{nout}}}{\frac{P_{sin}}{P_{nin}}} = \frac{\beta}{\gamma\,[1 - cos(\omega\tau)]} \tag{20}$$

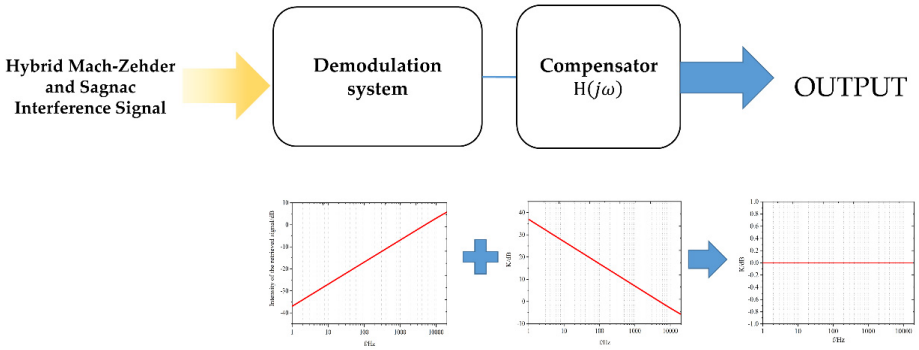

FIGURE 5. The demonstration of the time domain compensation for the interferometer system frequency.

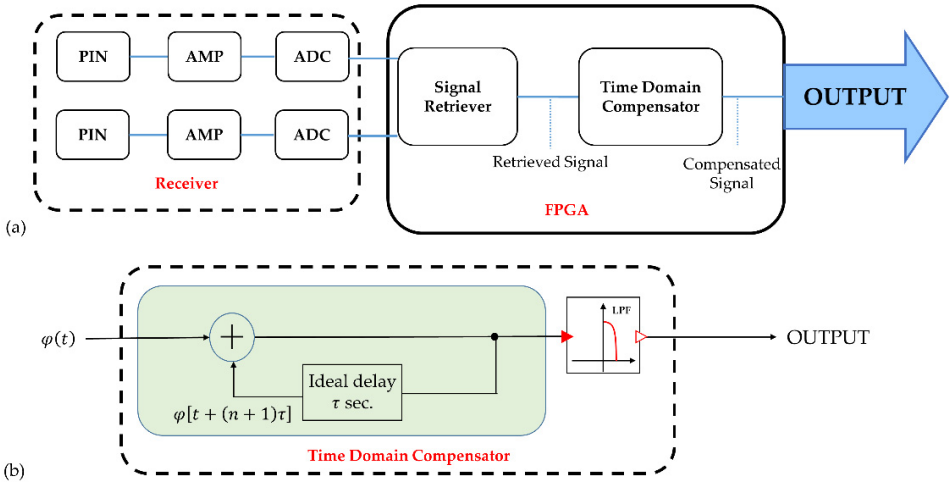

FIGURE 6. (a) Schematic diagram of demodulation and compensation circuit system; (b) The process diagram of the time domain compensator.

where we let $\beta = B\tau \cdot \sin(B\tau)$ and $\gamma = 2\pi^2 [1 - \cos(B\tau)]$ for simplicity. In the concerned frequency band, β and γ are both constant (the bandwidth B is 20 kHz and time delay τ is 10^{-5}s generally). The variation trend of SNIR with frequency ω is similar to Fig. 3. For the finite vibration signal, the SNR is improved, especially for low frequency signals. Moreover, the lower the signal frequency is, the more significant the improvement is.

III. EXPERIMENT

A. FREQUENCY RESPONSE OF THE COMPENSATED SYSTEM

The experimental construction of optical fiber differential interference system is conducted according to Fig. 1. The laser source is a WBLS with a central wave-length of 1550 nm and a bandwidth more than 30 nm. The length of FDL is 2×10^3 m. A piezoelectric ceramic transducer (PZT, Rps300/20$\times$ 18.20, of which frequency response is relatively flat in the frequency range) is used to simulate the vibration signal and the data sampling rate is 5 M Samples/s. The interference signal is received by PIN1 and PIN2, and then fed into an amplifier (AMP). After being sampled by an analog-to-digital converter (ADC), this interference signal is operated by data processing. With the exception of the connectors used in the sensing fiber, all the connections between optic fiber devices are fused.

Through the signal processing system, the interference signal is demodulated and the retrieved phase signal is entered into the time domain compensation system as shown in Fig. 6. Focus on the low frequency band, the frequency and amplitude of the vibration signal are changed respectively to investigate the improvement of the compensation scheme to low frequency signal.

By continuously reducing the frequency of the vibration signal input into the compensation system, we could figure out the low frequency signal measured by the improved system so as to maintain a high SNR. Fig. 7 shows the comparison of vibration signal before and after compensation,

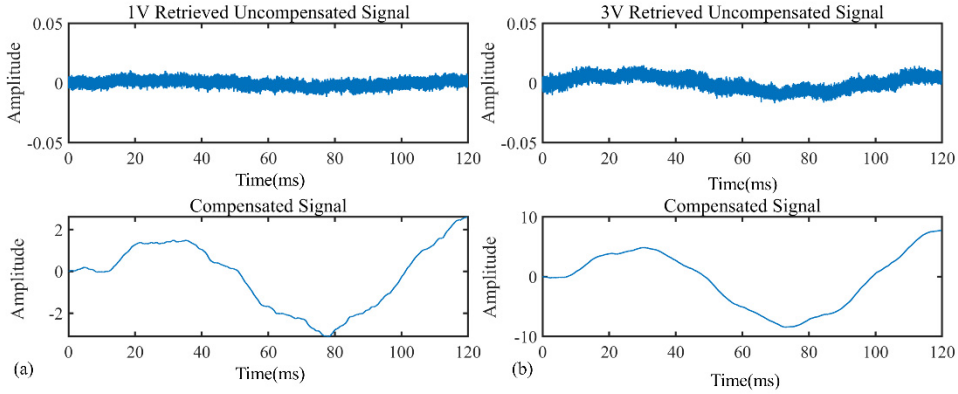

FIGURE 7. (a) The comparison of 10 Hz vibration signal with amplitude of 1V before and after compensation; (b) The comparison of 10 Hz vibration signal with amplitude of 3V before and after compensation.

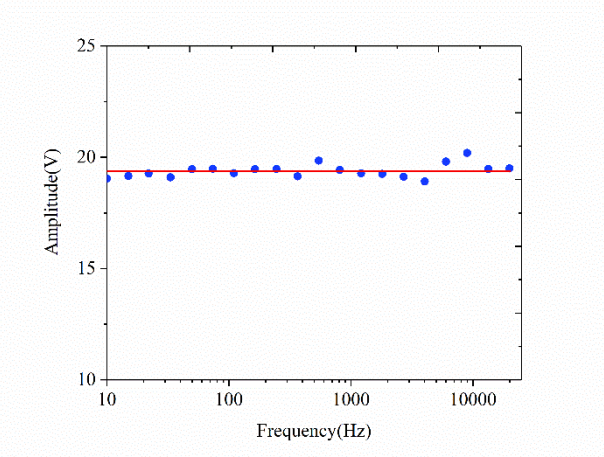

FIGURE 8. The frequency response of the time domain compensator to the vibration signal.

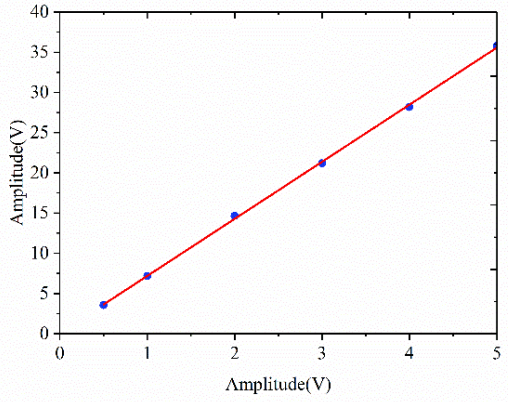

FIGURE 9. The response of the time domain compensator to the vibration signal with 30 Hz.

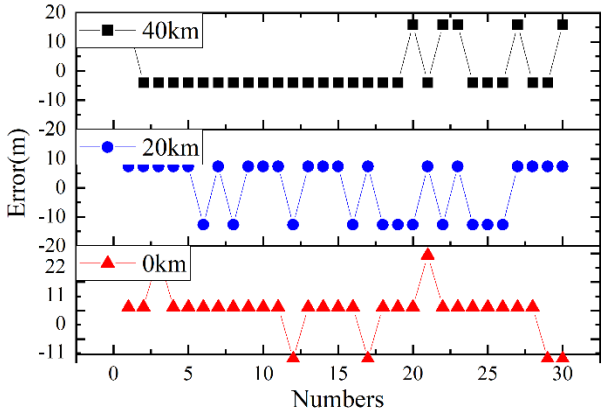

FIGURE 10. Positioning errors at the different positions.

of which the frequency is 10 Hz and the amplitude is 3 V and 1 V respectively. The amplitude of the compensated signal is significantly increased so that the signal waveform is clearly visible, which was completely overwhelmed by the higher frequency components before compensating. It is indicated from the measured signal that the signal frequency of 10 Hz with an amplitude of 1 V can be detected with high SNR by employing the compensator. The compensation system effectively extends the low frequency band of the differential phase detection system.

Fig. 8 shows the frequency response of the system adopting the time domain compensator when the vibration signal frequency with the amplitude of 5V changes in the range of 10 Hz to 20 kHz. It can be observed that after time domain compensation, the maximum frequency response difference is 4.09%, and the system has a good frequency response consistency within the frequency band of 10 Hz-20 kHz.

Maintaining the frequency as 30 Hz, the amplitude of the vibration signal varies from 0 to 5 V. The amplitude relationship between the compensated phase signal and the uncompensated vibration signal maintaining the vibration signal frequency as 30 Hz is shown in Fig. 9 where the abscissa is before compensation and the ordinate is after compensation. In the figure, the line is obtained by linear fitting. The results show that the output amplitude of the compensator has an exact linear relationship with the input amplitude.

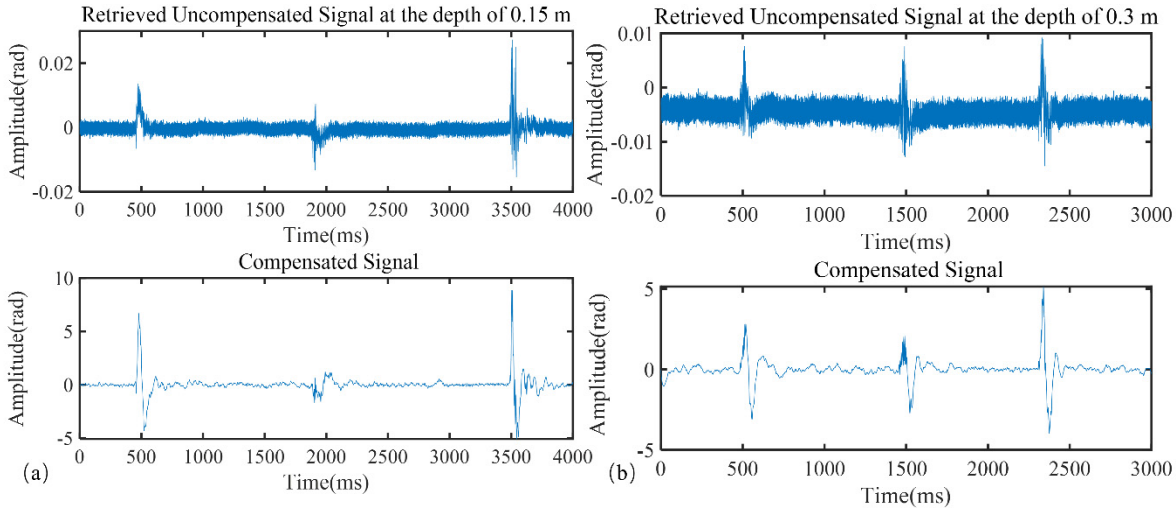

FIGURE 11. **(a) The comparison of walking signals detected on an optical fiber buried at a depth of 0.15 m before and after compensation. (b) The comparison of walking signals detected on an optical fiber buried at a depth of 0.3 m before and after compensation.**

B. LOCATION EXPERIMENT

In order to further verify the practicability of the time domain compensation scheme, a measurement of buried optical fiber was conducted. Since the soil will absorb the energy of the intrusion signals in practice, especially high-frequency components, more low-frequency signals are left transmitted to the buried pipelines. The experiment simulates the monitoring of buried pipelines, using optical fibers buried to a depth of 0.3 m and 0.15 m in the soil to measure external intrusion. The walking intrusion events are detected and compensated. After the walking signal has propagated for a certain distance in the soil, most of the remaining signals are low-frequency components. The low frequency compensation scheme significantly improves the SNR of the walking signals in Fig. 11, which is increased from 13.46 dB and 8.71 dB to 33.52 dB to 33.11 dB at the depth of 0.15 m and 0.3 m, respectively.

Then we verify the positioning ability of the system based on the buried optical fiber. From (3), after phase demodulation and compensation of the signals detected by PIN1 and PIN2, the autocorrelation algorithm is adopted to determine the sub-peak of autocorrelation function, and the location of the disturbance can be obtained. Three positions at the distances of 0 km, 20 km, and 40 km are selected as the test points and vibration is applied 30 times at each test point of the sensing fiber. It can be seen from Fig. 10 that the system has high positioning stability and the positioning error is within ± 20 m. Furthermore, the positioning accuracy can be improved by increasing the sampling rate.

IV. CONCLUSION

In this paper, we introduce an improved interferometer with a time domain compensation scheme to solve the problem that the differential phase detecting in M-Z and Sagnac hybrid optical fiber interference system has a poor low-frequency performance. This compensation scheme effectively improves the low frequency response of the optical fiber interference system. Experiments have proved that the system is capable of detecting low-frequency signals with 1 V 10 Hz and shows good frequency response consistency in the frequency band of 10 Hz-20 kHz. The SNR is improved by 22 dB approximately in the buried optical cable monitoring for external intrusion and the measured location error is within ± 20 m along the length of sensing fiber 40 km. Consequently, the compensation system can obtain effective detection at low frequency band, and the SNIR of the system increases with the decrease of the signal frequency. It is concluded that the interference system with a time domain compensation scheme not only retains the performance stability of the interference system, but also has great low-frequency characteristics, which enables high fidelity detection. Furthermore, it has extensive prospects of applications in low-frequency fields such as seismic waves, hydrophones, pipeline monitor and geological detection.

REFERENCES

[1] V. Ahsani, F. Ahmed, M. Jun, and C. Bradley, "Tapered fiber-optic Mach–Zehnder interferometer for ultra-high sensitivity measurement of refractive index," *Sensors*, vol. 19, no. 7, p. 1652, Apr. 2019.

[2] G. Allwood, G. Wild, and S. Hinckley, "Optical fiber sensors in physical intrusion detection systems: A review," *IEEE Sensors J.*, vol. 16, no. 14, pp. 5497–5509, Jul. 2016.

[3] T. G. Giallorenzi, J. A. Bucaro, and A. Dandridge, "Optical fiber sensor technology," *IEEE Trans. Microw. Theory Techn.*, vol. MTT-30, no. 4, pp. 472–511, Apr. 1982.

[4] J. Zhou, Y. Wang, C. Liao, B. Sun, J. He, G. Yin, S. Liu, Z. Li, G. Wang, X. Zhong, and J. Zhao, "Intensity modulated refractive index sensor based on optical fiber Michelson interferometer," *Sens. Actuators B, Chem.*, vol. 208, pp. 315–319, Mar. 2015.

[5] J.-H. Liou and C.-P. Yu, "All-fiber Mach–Zehnder interferometer based on two liquid infiltrations in a photonic crystal fiber," *Opt. Exp.*, vol. 23, no. 5, p. 6946, Mar. 2015.
[6] J. C. Juarez and H. F. Taylor, "Field test of a distributed fiber-optic intrusion sensor system for long perimeters," *Appl. Opt.*, vol. 46, no. 11, pp. 1968–1971, 2007.
[7] M. Deng, C.-P. Tang, T. Zhu, and Y.-J. Rao, "PCF-based Fabry–Pérot interferometric sensor for strain measurement at high temperatures," *IEEE Photon. Technol. Lett.*, vol. 23, no. 11, pp. 700–702, Jun. 1, 2011.
[8] Y. Wu, P. Bian, B. Jia, and Q. Xiao, "A novel Sagnac fiber optic sensor employing time delay estimation for distributed detection and location," *Proc. SPIE*, vol. 8896, pp. 88960A-1–88960A-8, Oct. 2013.
[9] Q. Mi, J. Bian, Z. Ye, and C. Wang, "Study of compensation demodulation method for fold Sagnac interferometer used in distributed disturbance sensing," *Opt. Eng.*, vol. 56, no. 11, p. 1, Nov. 2017.
[10] W. Yuan, B. Pang, J. Bo, and X. Qian, "Fiber optic line-based sensor employing time delay estimation for disturbance detection and location," *J. Lightw. Technol.*, vol. 32, no. 5, pp. 1032–1037, Mar. 1, 2014.
[11] A. A. Chtcherbakov, P. L. Swart, S. J. Spammer, and B. M. Lacquet, "Modified Sagnac/Mach–Zehnder interferometer for distributed disturbance sensing," *Microw. Opt. Technol. Lett.*, vol. 20, no. 1, pp. 34–36, Jan. 1999.
[12] S. J. Spammer, P. L. Swart, and A. A. Chtcherbakov, "Merged Sagnac–Michelson interferometer for distributed disturbance detection," *J. Lightw. Technol.*, vol. 15, no. 6, pp. 972–976, Jun. 1997.
[13] Z. Ye, C. Li, and C. Wang, "Ultra-long-distance (>160 km) distributed optic fiber vibration sensing system without an in-line repeater," *Appl. Opt.*, vol. 58, no. 13, pp. 3426–3431, 2019.
[14] C. Li, Y. Yan, and C. Wang, "Study on multi-time reflection induced by in-line fiber connector in engineering applied distributed single-fiber interferometer sensing system," *Microw. Opt. Technol. Lett.*, vol. 62, no. 9, pp. 3014–3022, Sep. 2020.
[15] Z. Ye, C. Li, and C. Wang, "A multichannel optic fiber sensing system based on hybrid Sagnac structure," *Microw. Opt. Technol. Lett.*, vol. 61, no. 11, pp. 2651–2656, Nov. 2019.
[16] M. Norgia, A. Pesatori, M. Tanelli, and M. Lovera, "Frequency compensation for a self-mixing interferometer," *IEEE Trans. Instrum. Meas.*, vol. 59, no. 5, pp. 1368–1374, May 2010.
[17] K. P. Koo, A. B. Tveten, and A. Dandridge, "Passive stabilization scheme for fiber interferometers using (3 × 3) fiber directional couplers," *Appl. Phys. Lett.*, vol. 41, no. 7, pp. 616–618, Oct. 1982.
[18] H. Wu, Y. Feng, H. Xu, and D. Zhao, "A new demodulation method to improve the sensitivity and dynamic range of fiber optic interferometric system," in *Proc. 9th Int. Conf. Opt. Commun. Netw. (ICOCN)*. Stevenage, U.K.: IET, 2010, pp. 70–72.
[19] G. Hong, B. Jia, and H. Tang, "Location of a wideband perturbation using a fiber Fox–Smith interferometer," *J. Lightw. Technol.*, vol. 25, no. 10, pp. 3057–3061, Oct. 2007.

YINGJIE WU received the B.S. degree from Fudan University, in 2019, where she is currently pursuing the M.S. degree. Her current research interests include optical interferometer and optical sensing.

CHURUI LI received the M.S. degree from Shanghai University, in 2007, and the Ph.D. degree from Fudan University, in 2013. His research interests include optical fiber sensing technology and signal processing.

HUANG TANG received the B.S., M.S., and Ph.D. degrees from Fudan University, Shanghai, China, in 1997, 2000, and 2010, respectively. Since 2010, he has been an Assistant Professor with Fudan University. His research interest includes fiber-optic sensing technology.

BO JIA received the Ph.D. degree from the University of Electronic Science and Technology of China, in 2000. He is currently a Professor with the Department of Material Science, Fudan University, Shanghai. His research interests include fiber-optic sensor and applications, optical communication, and so on.

CHAO WANG received the B.S. and Ph.D. degrees from Fudan University, in 2004 and 2009, respectively. He has been working at Fudan University, since 2009. His current research interests include optical fiber sensing technology and optical fiber communication.